NTNU – Trondheim
Norwegian University of
Science and Technology

Saturations Calculations Using Saturation-Height Modeling on the Well Mariana, offshore Lower Congo Basin

Saturation Height approachs

Dario Euclides Tenente
Pascoal

Petroleum Geosciences
Submission date: July 2015
Supervisor: Erik Skogen, IPT
Co-supervisor: Per Atle Olsen, Statoil

Norwegian University of Science and Technology
Department of Petroleum Engineering and Applied Geophysics

NTNU

Norwegian University of
Science and Technology

Saturations Calculations Using Saturation-Height Modeling on the Well Mariana, offshore Lower Congo Basin

Dário Euclides Tenente Pascoal

Petroleum Geosciences
Submission date: **July 2015**
Supervisor: **Erik Skogen, IPT**
Co-Supervisor: **Per Atle Olsen, STATOIL E&P**

Norwegian University of Science and Technology
Department of Petroleum Engineering and Applied Geophysics

NTNU

Norwegian University of
Science and Technology

Saturations Calculations Using Saturation-Height Modeling on the Well Mariana, offshore Lower Congo Basin

Dário Euclides Tenente Pascoal

1 Acknowledgements

My acknowledgements are primary engaged to the Only One able to be with me anywhere, God. Special recognitions to Per Atle Olsen, a patient and respectful supervisor from Statoil, for his guidance, ready availability and open comments to each line of the thesis. Secondly, thanks to Erick for accepting to be my supervisor from NTNU. I also acknowledge my dear fellow, Dondo Salomão, from Statoil ASA, for his support with data and answer to small questions during the thesis compilation.

A special thanks to the oil company, Statoil ASA, for all financial, technological and academic support for the practical part of the thesis become tangible. This appreciation is specially directed to Nils Janbu, for his dynamism to grant access to offices and material support from Statoil in Trondheim. It is also extended to all people in Luanda that struggle to grant it. Yet, special thanks to Jose Martinez and Manuel A. Seque, from Statoil Luanda, who were always present for any additional support.

My appreciation goes toward all members of the program ANTHEI, mentors and colleagues from Angola, Tanzania and Mozambique. To the mentors I direct my singular gratitude firstly to UAN (Agostinho Neto University) because all started from there, especially to Emidio Silva, from Faculty of Engineering. Secondly a distinct gratefulness to NTNU, especially the Head of the Department, Egil Tjaland, and his team (in Special, Tone Sanne, Madelein and Anne Lise) for all support and emails eagerly responded. To all professors from NTNU that granted a jump to my scientific knowledge, my big thanks.

Finally, I address great thanks to my parents which are always the beginning of all past, present and future achievements. Also to my notable helpmate, Wilma Pascoal, for her comprehension, patient and support (without which, these two years would be a torture). To my second fathers, Anibal Cabange and André Buta Neto, for psychological and emotional support towards family challenges, during my absence from Angola. To all my friends, closer than any brother, that decided to sacrifice parts of their goals to support my coming to this master challenge.

2 Abstracto

Cálculos de saturações tem sido, por muitos anos, objeto de grande importância para a indústria do petróleo. Muitas literaturas mostram diferentes esforços empíricos e científicos para produzir funções de saturação robustas que possam incluir quase todas as propriedades das rochas e interação entre os fluidos. Essas características são na sua maioria porosidade, resistividade e constants que indicam o tipo e particularidades da formação. Saturação-Altura (SwH) funções podem comportar estas propriedades, incluindo a permeabilidade, mas baseia-se na variação de saturação em função da altura acima do nivel-livre de água (HAFWL) ou pressão capilar. Mapeamento de saturação de água em partes da formação, distantes do poço , por exemplo em geo-modelos é o principal objetivo da modelagem de funções de Saturação-Altura. Estas são importantes porque podem influenciar fortemente nos cálculos de STOIIP ou GIIP de um reservatório e realçar a decisão da profundidade para perfuração. Muitos métodos para funções SwH estão disponíveis na literatura. O objetivo desta tese baseia-se na aplicação de alguns desses métodos para um determinado domínio e para discutir a conformidade e disparidade com o modelo de saturação já aplicada ao campo. Para isso foram utilizados e processados dados de registro do poço, Mariana, perfurado dentro da Bacia do Baixo Congo, em águas ultra-profundas, no offshore de Angola. Dois modelos de equação de Saturação-Altura foram aplicados ao poço Mariana os quais mostraram dar resultados fiáveis, método FOIL (Cuddy) e Leverett (J). Ambos os métodos mostraram-se razoável para o cálculo Saturação do Poço. O Método Cuddy revelou-se sobrestimar, enquanto Leverett (J) mostrou a subestimar os resultados de saturação, quando comparado com a referência de saturação utilizado anteriormente no poço.

3 Abstract

Saturations calculations have been, for many years, object of high importance for the oil industry. Many literatures show different empirical and scientific efforts to produce robust saturations functions which attempt to address almost all properties of the rocks and fluid interaction. These features are mostly porosity, resistivity and factors that address the type and particularities of the formation. Saturation Height (SwH) functions may address all these properties, including permeability, but relies on the variation of saturation as function of the Height Above the Free Water Level (HAFWL) or capillary pressure. Mapping of water saturation away from the wellbore in for instance geo-models is the main purpose of saturation height modeling. Saturations height functions are important as can highly influence the STOIIP or GIIP calculations for a reservoir and enhance the perforation depth decision. Many methods for SwH functions are available in the literature. The purpose of this thesis relies on the application of some of these methods to a given field and to discuss conformity and disparity with the saturation model already applied to the field. For that were used and processed in the software Geolog raw log data of a well, Mariana, drilled within the Lower Congo Basin Ultra-deep-water province, offshore of Angola. Two saturation-height models equation were applied to the well Mariana to compute water saturations which showed to give reliable results, FOIL method (Cuddy) and Leverett (J) Function. Both methods showed to be reasonable for the Saturations calculation of the Well. Cuddy Method revealed to overestimate, whilst Leverett (J) showed to underestimate the saturations results, when compared to the Saturation reference used previously in the well.

Contents

4 List of figures

5 Acronyms

GIIP	Gas Initial in Place
HAFWL	Height Above Free Water Level
JF	Leverett J Function
Pc	Capillary Pressure
PHITT	Total Porosity (computed by the Oil Company)
STOIIP	Stock Tank Oil Initial In Place
SwH	Water Saturation Height
DNS	Density-Neutron curves separation
TVD	True Vertical Depth
TVDSS	True Vertical Depth Subsea

6 Introduction

Petrophysical analysis has as main goals to produce information that facilitate on defining the STOIIP or GIIP of reservoirs. This analysis includes mainly porosity, Saturation, Net to gross. While Net to Gross, porosity and permeability are readily mapable quantities the saturation needs special considerations to be extrapolated from the well. Mapping of water saturation away from the wellbore in for instance geo-models is the main purpose of saturation height modeling. Saturations are affected by factor as Rw or Rt values from log measurements, which are mostly affected by clay content, shoulder bed effect, salinity and wellbore stability. The *m* and *n*, cementation and saturation exponents respectively, have also great effect in the water saturations values (Walther, 1967; Hamada and Alsughayer, 2001). The Saturation also varies as function of the capillary entry pressure all over the formation, which is controlled by the wettability interfacial tension and pore geometry (Harrison and Jiang, 2001). The later has been object of many studies along the years and different approach has been performed to acquire better answers. One reason why it has been studied is the fact that has direct influence on the calculation of the amount of oil or gas in the formations or in a field to be explored (when many wells are evaluated). This means that robust SwH Functions can be used for prediction of saturation at any part of the reservoir above the free water level, usually considering rock qualities variation. Former studies show that SwH functions can be acquired through two principal categories: Core analysis data and Log analysis data. Many Literatures around these two different methods are found (Wiltgen et al. 2003; Skelt and Harrison, 1995). The purpose of this thesis relies on the application of some of these methods to a given field and to discuss conformity and disparity with the saturation model already applied to the field.

6.1 Fundamentals Concepts

In reservoirs the fluids are initially in equilibrium within the porous space of the rocks. Two non-miscible fluids sharing the same porous space tend to occupy different positions depending on their density contrast. Three main forces influence in the amount of each fluid in the reservoir: gravity (buoyancy) force, an external force (flow coming from an aquifer near the reservoir, for example) and interfacial forces. The effect of the latter one on the fluid amount and interface

position is the one to be considered in this dissertation. Thus some main concepts are important to be described.

6.2 Capillary Pressure and Wettability

The Capillary pressure may be explained by the interaction between fluid-fluid and fluids-solids causing a fluid pressure difference. Consider a rock which pore space filled with two immiscible fluids. Each fluid will interact with the pore surface (solids) and with neighbor fluid sharing the same porous space. The interaction effect will depend on the inter-molecular attraction (forces): the fluid-fluid interaction, will give place a *surface tension*; the solid surface area occupied by the fluids depending on their molecular affinity to the solid. The degree of affinity is defined by the angle formed between the fluids interface and the solid surface, which express the *wettability* of the fluid. The less the angle, the greater is the wettability of the fluid. Drainage occurs when hydrocarbon migrates into a reservoir and displaces water. In order to displace water hydrocarbon need to overcome the displacement pressure of the rock set up by the capillary pressure.

6.3 Free Water Level (FWL) and Fluid Contacts

The free water level, FWL in a water wet rock, is defined as the point below fluid contact which capillary pressure is zero. It is also used as reference in many Saturation-Height modeling functions which above such the height is measured. Above the FWL where capillary pressure is different from zero hydrocarbons can displace water. In logging analysis, formation pressure data plotted against True Vertical Depth are used to predict free water level by checking the points where fluid pressure gradient lines are crossed. For the fluid contacts the inference is addressed differently as its position may vary as function of the pore size: small pore-sized rocks trend to have fluid contact a bit further above from the FWL comparatively to large pore-sized rocks. Also, it can be obscured by shale beds in a shaly sand sequence, or almost unpredictable in very thin layers.

6.4 Fluid Saturation

The amount of fluid within the porous space of a rock defines the saturation of a reservoir. There can be found three types of fluid in a reservoir: Water, Oil and Gas. The sum of the three fluids will correspond to the total pore volume and the saturation of each fluid will indicate the individual contribution of each fluid to the total.

6.4.1 Water Saturation (Sw)

Water saturation corresponds to the ratio of water volume to pore volume of a rock sample. The water fraction that cannot be displaced by capillary forces and is normally attached to the matrix of the rock is often named *irreducible water saturation*. There are many different approaches for calculating water saturations along the well-bore. The most common, in petrophysics field, is by the well know Archie´s Formula.

$$Sw^n = \frac{Rw*a}{\emptyset^m*Rt} \quad (1)$$

6.5 Saturation-Height Functions (SwH)

Several studies concerning to Saturation Height were developed through the years, which gave place to different methods to compute Sw through SwH modeling. The available literature divides them mostly into two types: those based on capillary curve averaging and those log-based methods. A third type that integrates both has being also considered. The next few lines shall describe some of them.

6.5.1 Classical Functions (Leverett Function)

A paper produced by Leverett (1940) describes the Capillary behavior in porous solid. His objective was considering applications of Thermodynamic and physical principles to Static and Dynamic behavior of the fluid mixture. Differently from the empirical ones, he used rock physics properties to elaborate a dimensionless function which attempt to generate universal curve. He related the Interfacial Curvature definition and its relation with three important parameters: Capillary pressure, Height and Saturation. Leverett argued that when two fluids fill a pore they

form an interface, which shape is function of the tension between the fluids that result in a differential pressure across the interface. This first relationship is described by the equation:

$$Pc = \gamma\left(\frac{1}{R1}+\frac{1}{R2}\right) \quad (2)$$

Where $\boldsymbol{\gamma}$ is the Interfacial tension, $\boldsymbol{Pc}$ is the capillary pressure, $\left(\frac{\mathbf{1}}{\boldsymbol{R1}}+\frac{\mathbf{1}}{\boldsymbol{R2}}\right)$ correspond to the main curvature of the surface and R1 and R2 are the principal radii of the curvature.

The second relationship relies on the assumption that fluids in reservoir are initially in *substantial capillary equilibrium*. Fluids in the reservoir occupy different individual vertical position. Their position depends, among other external factors, of the fluid density contrast. Therefore, the interface may be described as result of the difference between the densities of the fluids, the gravity and their depth position difference in the reservoir. This relationship describes the well-known capillary pressure equation shown below. This equation states equilibrium between the hydrostatic pressure and the buoyance.

$$dPc = dPo - dPw = \Delta\rho_{wo} g dh \quad (3)$$

So, assuming capillary equilibrium is the same as saying there would be no curvature at the interface or zero value on the capillary pressure.

$$Pc = \Delta\rho_{wo} gh = \gamma\left(\frac{1}{R1}+\frac{1}{R2}\right) \quad (4)$$

This can be also written:

$$\left(\frac{1}{R1}+\frac{1}{R2}\right) = \frac{\Delta\rho_{wo} g h}{\gamma} \quad (5)$$

Where $\boldsymbol{\Delta\rho_{wo}}$ is the density difference between water and oil, *h* is the vertical distance of the interface above the free liquid surface and *g* is the gravitational constant. Leverett made some important considerations of equation (5) from which the most relevant for this study is that it could be *a direct means of estimating the maximum difference pressure that may exist in a virgin reservoir.*

The last relationship relies on assumptions of a considerable contribution on the curvature of the oil-water interface, from the dimension of the pore space and the fraction of the fluid phase existent within the pore. He also took into consideration the minimum pressure differential enough to displace water from the water saturated sand, Displacement Pressure. A two phase experiment (drainage and imbibition) was performed and measured the resultant *Sw* of 2 different rocks at different capillary pressures, by letting water and air come to a capillary equilibrium. Peculiar rock parameters, permeability and porosity, were related by $\sqrt{\frac{k}{\emptyset}}$, and bounded to equation (5). The right hand side became then: $\frac{\Delta\rho_{wo}g\mathrm{h}}{\gamma}\sqrt{\frac{k}{\emptyset}}$

Ibrahim A. et al (1992) made a determination of relative permeability curves in tight gas sands using log data and culminate with a useful approach using the Leverett equation:

$$\mathrm{J(Sw)} = \frac{\Delta\rho_{wo}g\mathrm{h}}{\gamma}\sqrt{\frac{k}{\emptyset}} \tag{6}$$

And taking into account the wettability effects was included the contact angle, θ into ***J(Sw)***

$$\mathrm{J(Sw)} = \frac{\Delta\rho_{wo}g\mathrm{h}}{\cos\theta\,\gamma} * \sqrt{\frac{k}{\emptyset}} \tag{7}$$

They plotted the J(Sw) calculated against *Sw* data in a log-log scale and realized a nearly linear fit. The best reflects the equation:

$$\mathrm{J(Sw)} = \frac{\alpha}{Sw^{\beta}} \tag{8}$$

Where β and α, are coefficients. The capillary pressure, Pc, was related to FWL by:

$$Pc = \Delta\rho wog\mathrm{h}_{\mathrm{FWL}} \tag{9}$$

Where, $\boldsymbol{h_{FWL}}$ indicates the height above the free water level. By rearranging the equations above and solving for $\boldsymbol{Sw^{\beta}}$:

$$Sw^{\beta} = \frac{\cos\theta\,\gamma}{\Delta\rho_{wo} g h_{FWL}} \sqrt{\frac{\emptyset}{k}} \tag{10}$$

A plot of the new form of equation (5) versus *Sw*, results in the known J function or simply *J(Sw)*, which is dimensionless. The solution of this function is verified, in a log-log scale, by the equation (6):

$$\log Sw = A + B \log(J) \tag{11}$$

However, this method is dependent much of the history and flow of the system (Leverett, 1942) and as each rock has different geological history, this method gives reliable result if evaluating only a single type of rock. Fig. 1 shows typical curve produced by Leverett function.

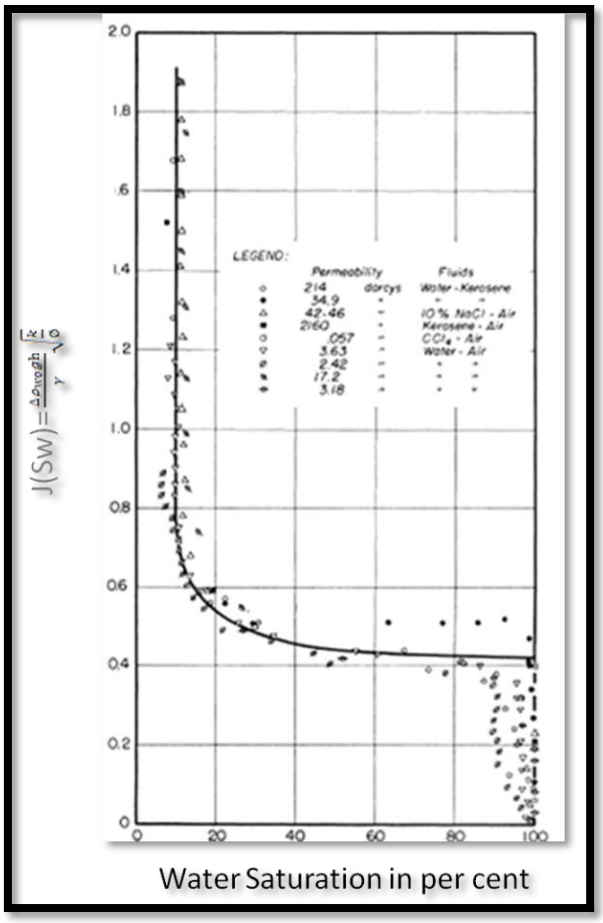

Figure 1 - Example of the Leverett Curve (Leverett, 1942)

6.5.2 FOIL functions

Other authors calculate the Swh based in the Bulk volume of water, which received the name FOIL functions (Wiltgen et al., 2003; Cuddy et al., 1993)

The most known FOIL equation is the function produced by Cuddy et al. (1993). They created a function virtually independent of porosity and permeability based on the bulk volume of water

and FWL. The derivation is simpler than the classic ones. It starts by using the Ibrahim´s SwH relationship and uses the BVW definition from *Sw* and porosity:

$$\mathrm{BVW} = Sw * \emptyset \tag{12}$$

The porosity independence of Cuddy model could be shown by assuming the Sw calculated from equation (1). However, electrical properties of the rock may always influence the model results (see explanation in the Appendix). The BVW of water can be linearly related to the HAFWL when plotted in a log-log scale. The relation can be verified by the equation below.

$$BVW = A * (HAFWL)^B \tag{14}$$

Where, A and B are coefficients. Fig. 2 shows the final FOIL curve computed by Cuddy.

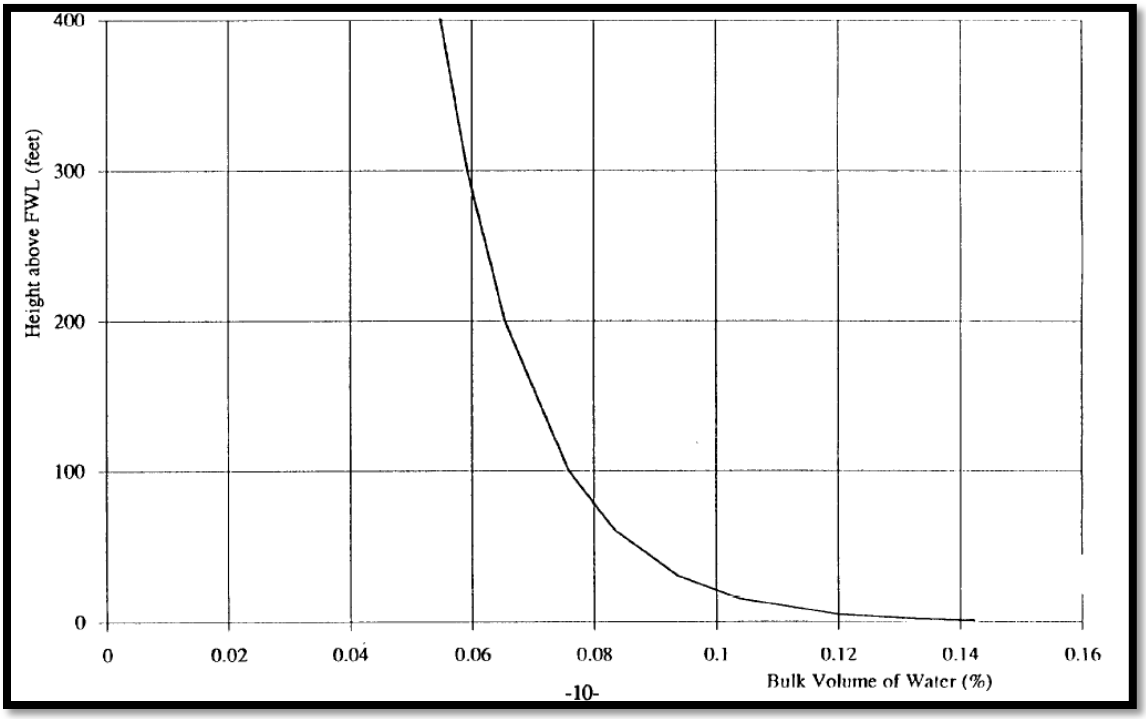

Figure 2 - Example of foil function (Cuddy et al., 1993)

6.5.3 Empirical Functions

These functions are based on porosity band. This means that a branch of Swh curves were plotted as function of some porosity averages measured in the same rock. The mains weakness of these functions, as pointed by Cuddy (1993), were that even though being consistent with the capillary pressure theory, were mathematically inconsistent, the data for porosity bands were not equally distributed, the vertical offset between the Swh curves needed to be known before the Swh calculations and did not have into account physical properties of the rocks. Some examples of these functions and typical curve are shown by Cuddy's paper (Cuddy et al., 1993).

Many other approaches functions exist for computing Swh (Wiltgen and Owen, 2003). Below is shown some of them:

Lambda Functions: $\lambda = e^{a+b*\ln(\emptyset_e/100)}$; $Sw = (Pc/Pe)^{-\lambda}$

Johnson "Pseudo-Permeability": $\log(Sw_n) = A * logK + (a * Pc^b)$

Guthrie Polynomial: $Sw = a_1\emptyset + a_1 logK + C$

Some of these functions require data of more than 1 well or core set (Pseudo-permeability) as they are based on linear correlation of permeability with same capillary pressure values, whilst others more complex to be implemented (Guthrie).

7 Methodology

The analysis of the parameters previously described (in the previous chapter) was applied to the well described below. The choice of which data to work with was based on the necessary elements for Saturation Height equations to be computed. These were mainly parameters that describe rock qualities (porosity and permeability - through log and core data); fluid physical properties (pressures - through pressure test data and fluid density difference assumptions) and Fluid-rock interactions (contact angle, interfacial tension, and fluid saturations). Rock quality parameters were ideally calibrated to core data, while others were simply assumed.

7.1 General well information

The well Mariana was drilled within the Lower Congo Basin Ultra-deep-water province, offshore of Angola. The drilled structure *is highly inclined Salt flank from Oligocene which clastics have an overlying Miocene regional seal truncated up dip against a salt diaper* (Geological Report, 2004). The main objective was to verify and prove the presence of two good quality oil reserves. Previous information acquired from other wells drilled in the same zone indicated that the targets consisted mainly of turbidity channels and associated overbank facies. This directional well has a projected deviation of approximately 46 degrees (maximum deviation) and 4359m TVD (4955 MD) of bottom depth with a water depth around 1632m. Formation targets were intercepted up structure from a depth of about 3484.m TVD (wellsite final report, 2004). **Fig. 3** shows a sketch of the well design. For this particular project it will be looked only the features within the Primary Target. It contains water, Oil and Gas in the reservoir. The saturation height modelling will be focused on the Water-Oil zone only and a small gas gap is neglected in the analysis (WOC and calculation of the volume of reserves). This well was particularly chosen because of the existence of a reported Water-Oil Contact (WOC) and drilling conditions. As reported and shown in the **Fig. 3**, it was drilled in severe safety conditions and to drill another well (or wells) near it that could address the rock properties at salt diaper direction is extremely risky and is less probable to happen. Thus, a SH model built from the Mariana well could be extrapolated to reservoir zones where data acquisition will be even more challenging.

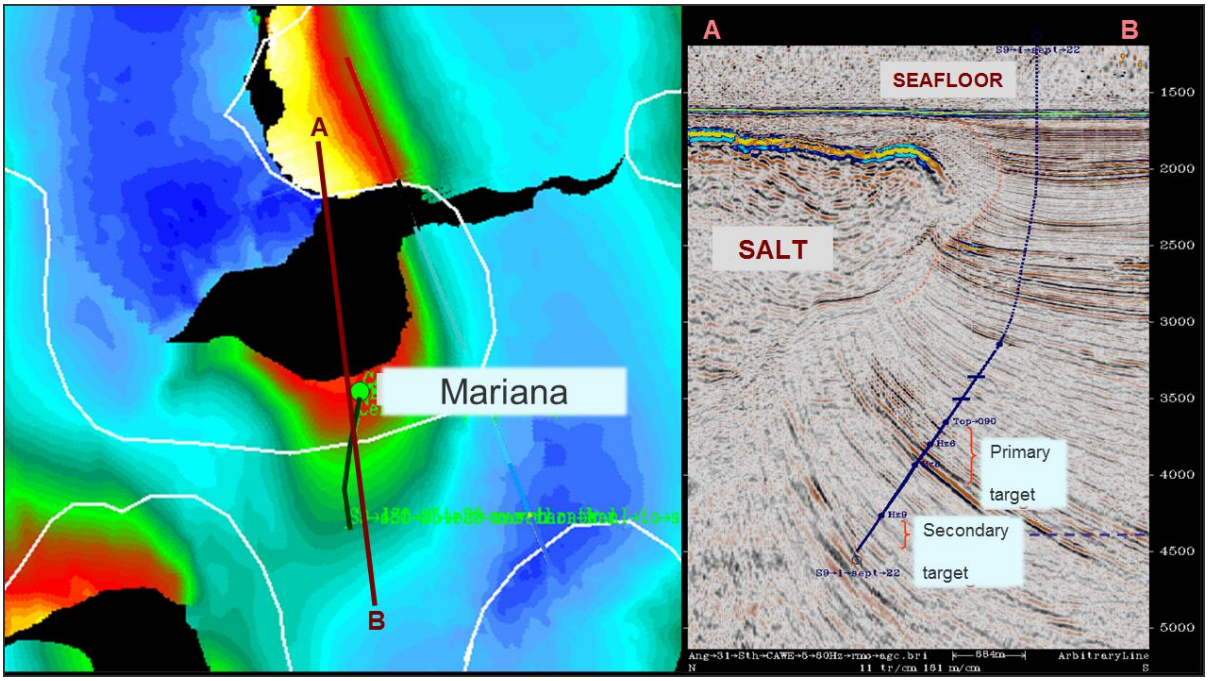

Figure 3 – At the left is shown the structure map of Well Mariana and location depth. On the right a general seismic cross section of the well trajectory (source: Core Sedimentology Report, 2005)

7.2 Well Data and Software

Raw data from well logs were available and processed through the software Geolog 7.1. These data consisted of some basic and special log data measurements as a function of measured depth: GR, calipers, resistivity, neutron, density, Spectral GR and NMR. Interpretation of water saturation, porosity, shale volume and Sandflag, was also available. The software was particularly important since it permitted import and processing of the raw data, to build up real and synthetic log curves, create formation filters (sandflag) and find Free Water Level (FWL), creating plots, to calibrate some raw data to core data, apply and manipulate different equations including build up SwH synthetic models.

7.3 Core Data

Routine core analysis as porosity, permeability and grain density was available for calibration of porosity and permeability logs. In total 34 core plugs from the zone of interest were considered suitable for analysis (no fracture or damages).

7.4 Lithology Analysis

The basic log combination principles such as DNS and full association analysis of the formation logs such as NMR, Pef, GR and Spectral GR were essential for quick and more detailed analysis of lithological sequence. Sedimentological reports of the core collected were available and in addition to the logs data they established fundamental bases for lithological comparative interpretation. Fig.6 shows the Density-Neutron curve separation analysis, typical of sand (yellow) and shale (green) sequence. It is supported by the GR curve values and NMR measurement. The caliper and Bit Size (BS) curve separation shows that in the most of the cases, the formations present to be unconsolidated. Thus, a fair conclusion is that the well was drilled in sand-shale sequences which sands vary between consolidated and unconsolidated.

7.5 Filter (Vshale and Sandflag)

Further studies of the well revealed the existence of some clay minerals (such as Montmorillonite and Illite) that could affect the results for a water saturation model of the well based on clean sand (Well Report, 2005; Pascoal, 2014). However the studies were qualitative rather than quantitative and no conclusive clay effect on water saturation computation has been considered. But, for avoiding shale bed analysis inclusions on the calculations, coherent filter was created. This filter is a Sandflag Log created through Vshale. It was computed only using well log information collected within the interval of interest and taking into consideration hole-size challenging effect on GR. Within the zone of interest, GR values vary between 16API (the GRmin of the entire well, coincidently) and 98API and the Gamma Ray Index (IGR) was calculated only in view of Vsh = (((GR-16) / (98-16))). Although a linear IGR relationship to Vsh alone trend to overestimate Vsh content (Doveton, 2014), it does not disagree much from the geological reports comments and from the NMR bound fluid trend concerning to formation type

and clay mineral presence. A Vshale curve of the reservoir, computed by the petrophysics staff of the company, was available and used as guide for calibration. Sandflag was computed through the relation (IFC (VSH_WO<0.30, 1, 0)) meaning that data analysis were performed only within sand formations which shale volume computed were less than 30% and therefore considered as clean.

7.6 Porosity

The porosity used for computing SwH was verified through 3 steps. First, equation (15) was used to build two log porosity curves (DPHI and FBPHI) considering unique formation density (Rho_{matrix}=2.65) but different fluid density. For the first curve was used Rho_{water}=1 through the entire well. For the second curve was used RHO_FLUID =1.01 and 0.85 (the same values reported for Pre-Test analysis) within the zone of interest. The fluids depth boundary was established slightly above the FWL point acquired from the TVDSS/Formation-Pressure crossplot (**Fig. 5**). Secondly, both curves were plotted against core porosity (CPOR). **Fig. 15** (Appendix) shows that no much difference can be noticed between both porosity logs when correlated to CPOR in a crossplot. However, when are placed in a log plot layout with the CPOR, better fit seems to be seen on DPHI (**Fig. 4**, tracks 3 and 5 from left). Finally, both curves were displayed together with LFP_PHITT (company porosity data, blue curve) and is evident a good match of both curves to CPOR and with LFP_PHIT, thus was decided to use LFP_PHITT for SwH computation, as it showed reliable Calibration.

$$\varphi = Rho_{matrix} - Rho_{log}/Rho_{matrix} - \text{RHO\_FLUID} \quad (15)$$

7.7 Permeability

An available core Klinkenberg Permeability (KP – black asterisk in **Fig. 4**) was calibrated to Core Porosity data and was essential for Computation of the SwH functions. **Fig. 4** displays the CPOR versus KP crossplot (at the right) where prominent clustered data is shown and naturally a reasonable calibration is expected from the correlation. A regression line was applied to build up interpolated log permeability. As LFP_PHITT porosity showed to match almost perfectly with CPOR and fitted well to the computed DPHI, it was decided to use it as variable in equation (16).

This log permeability, calculated in the form of equation (16), became then the one used for SwH computation, as it matched reasonable to core permeability (KP). A curve trend variation of both, core (KP) and the log permeability (the red curve on the center of the layout), is displayed in the Fig. 4 (track 4, from left) and acceptable match can be assumed, for most of the points, to KP.

$$K_{log3} = 10^{(a+b*PHITT)} \tag{16}$$

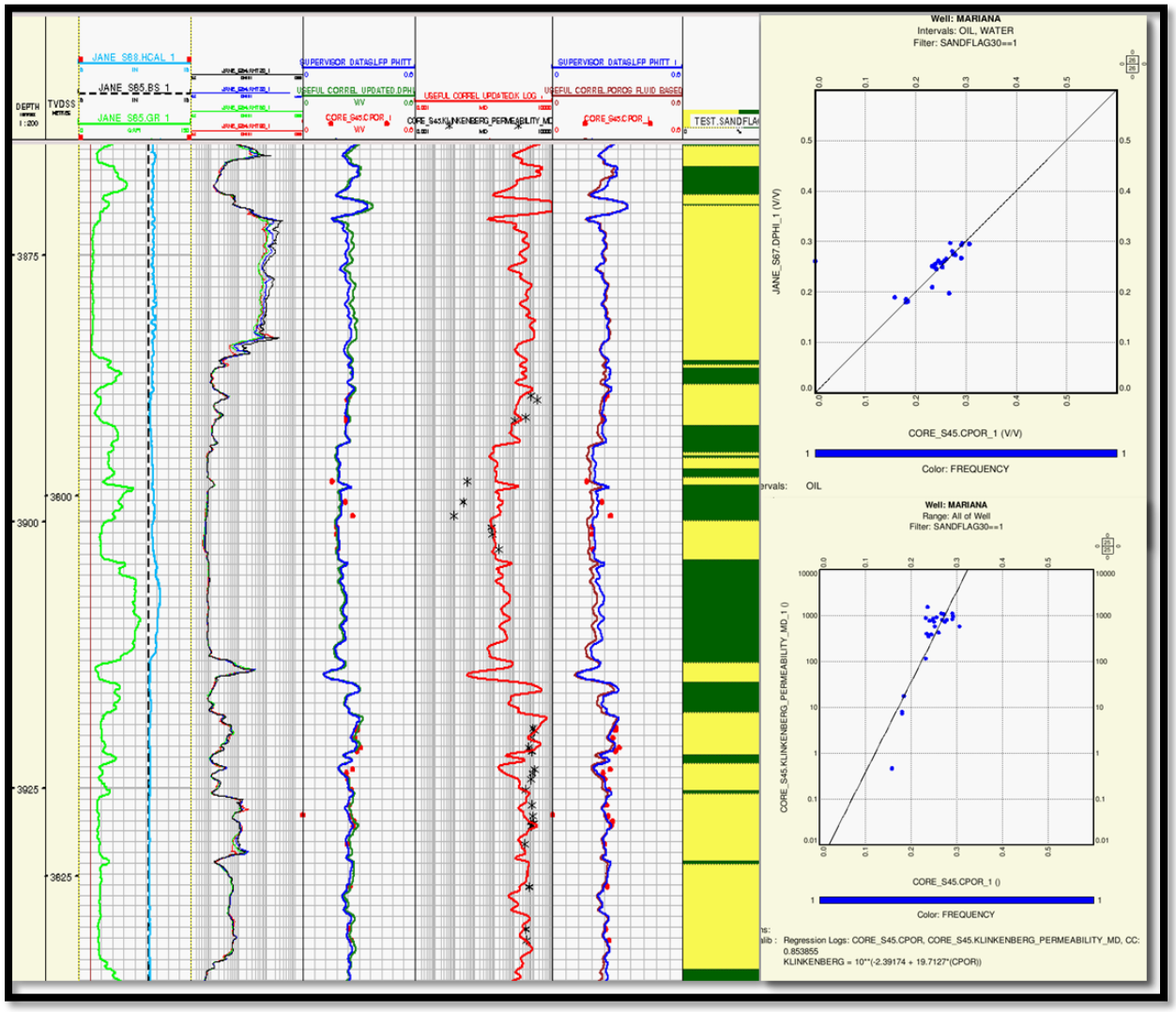

Figure 4 - Layout showing log porosity and permeability curve fit to core data (red and black dots, respectively). The plot on top-right indicates the calibration for porosity whilst the one below indicate for permeability

7.8 Free Water Level

A TVDSS vs. Formation pressure (FP) crossplot was built from available pretest analysis data. Similarly to core analysis and Resistivity logs, these data were particularly important and fundamental for defining the zone of interest. Fig. 5 shows the pressure data points. Gradient lines were applied and it shows that both gradient lines crossed at a depth between 3655 and

3658m (TVDSS), where is assumed to be the FWL point, however this point is masked by shale bed. The HAFWL was calculated by using the relation: IF ((3655-TVDSS)>0, (3655-TVDSS), 0), which means that all the depth points greater than 3655 were placed to zero (0). Both SwH models were compared with water saturation curve computed by the Oil Company (LFP_SWT). It is commonly assumed the WOC to be few meters above the FWL. As seen in **Fig. 13,** the FWL, blue dashed line, indicates that the fluid contact is much unclear as it is masked by shale beds. Then, not taken into account the exact WOC location point, were roughly built fluid zones, oil and water zone, for helping to restrict the analysis of the well.

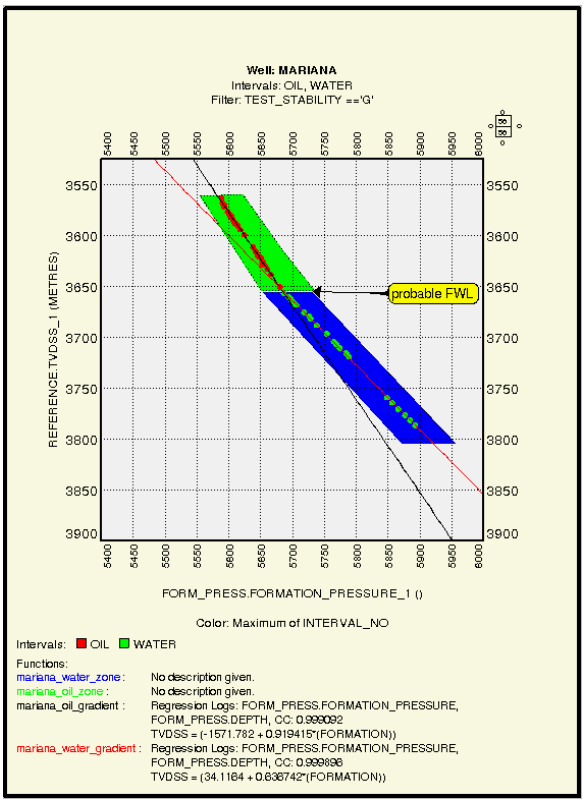

Figure 5 - Crossplot showing the pressure gradients lines and the limits of the zone of interest indicated by the fluid zones

7.9 Capillary Pressure

Capillary pressure was calculated as the buoyancy pressure assuming equilibrium with capillary pressure. The densities assumed were 1010 and 850 (kg/m^3) for water and oil, respectively; 9.8

m/s^2 for the gravitational constant (g) and the height (h) corresponds to vertical distance above the assumed free water level (HAFWL). Capillary Pressure versus Sw crossplot was used to identify Pc basic concept of pore size distribution and displacement pressure. No core analyses of capillary pressure versus core saturation were available.

7.10 Water Saturation

A water saturation log was available and served as reference for the saturation height model, but lacked information on how it was computed. Thus, a first attempt was to compute a Sw curve using scientifically trusted method to address the possible effects from logs measurements to the given Sw. A first guess was to use the well-known Archie´s formula (equation. 1). Then, its necessary inputs, Rw, a, φ, m, n and Rt, to compute it was the main task. *Rw* was computed by performing Porosity (PHITT) versus deep Resistivity (AHT90) Pickett plot. Water zone was filtered (by Vsh<30) and the 100% water filled sand line was adjusted to correspond the nearest sand interval below oil zone (see red dashed line **Fig. 16**). Constant *a,* was set to 1, as commonly used for sand rocks, as well as n=2 (Hamada et al., 2001). Constant *m* was adjusted to the picket plot. The best fit was m=1.7 with final result of Rw=0.029 Ohm. **Fig.6** shows 2 curves, LFP_SWT (red) and SW from Archie (black), both on the track four from left to the right, and can be noticed reasonably good curve trend fits. Both curves shows best linear correlation in low water saturated sand. Thus, it is assumed that this reference LFP_SWT curve was computed using Archie´s and the curves differences may be resultant from the differences in the input parameters. Furthermore, resistivity effects, such as shoulder bed effects, and others Archie's limitation can be expected from all calculations which it is included.

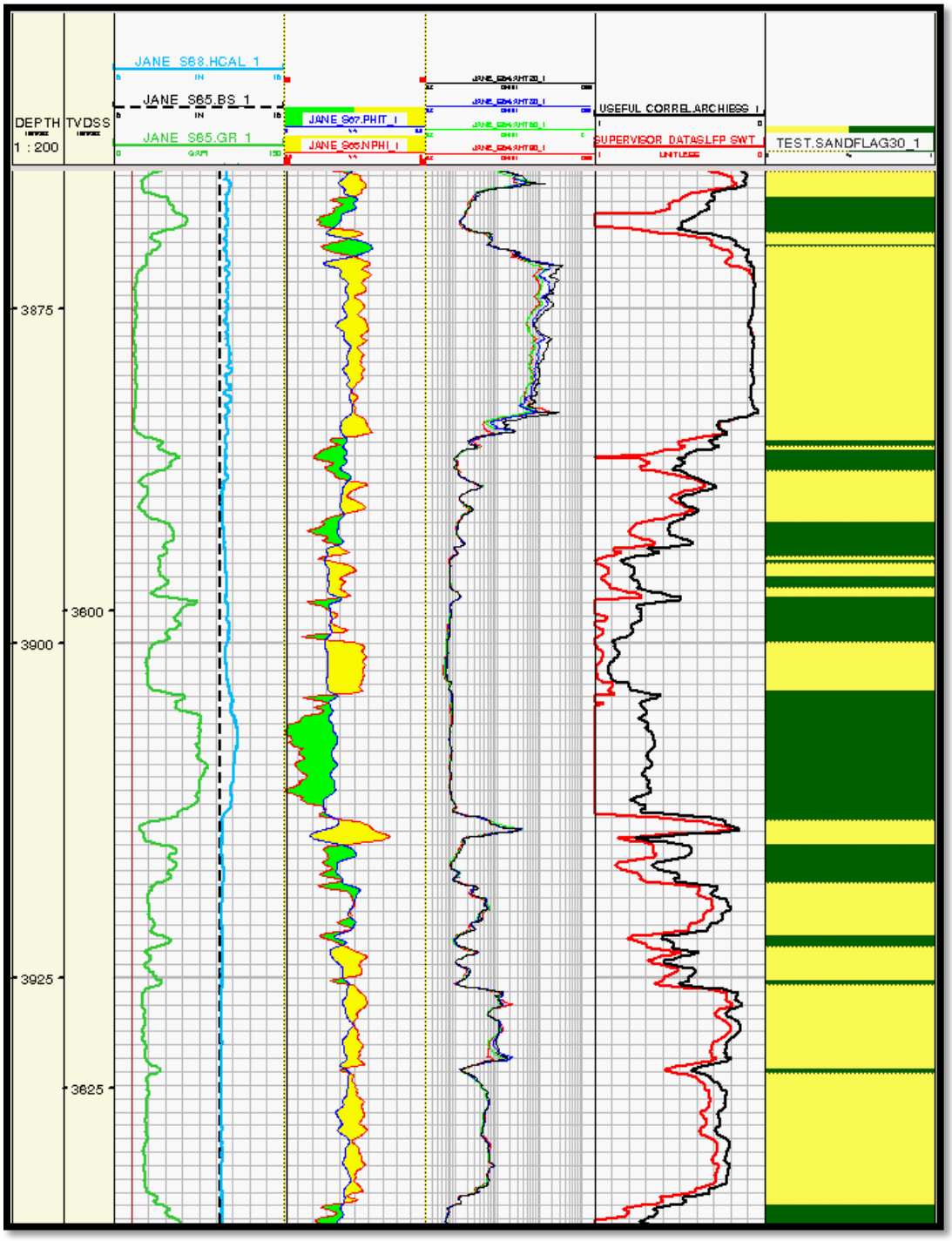

Figure 6 - Layout showing the verification of the reference Sw, computed by the company, in the zone of interest (track 4). The Depths shown here are Measure Depth and True Vertical Depth Subsea.

8 Results and Observations

Two Saturation height models were tested using data from the single well described above. One relates the variation of the water saturation as function of the rock quality, J_Function, while other relates the bulk volume of water (BVW), and therefore the porosity independence, with the height above free water level (HAFWL). In both cases then, the general assumption is that fluids are in capillary equilibrium in the reservoir.

8.1 Leverett J_Function

Leverett-J function can be established both from laboratory and log data. For surficial tension (γ) was assumed 30 dyne/cm whilst for contact angle (θ) was 30 degree. For capillary pressure were used results from equation (3) in Bars. The final results were achieved by using equation (8). A conversion factor of 3.14 was used to address all unit differences. **Fig. 7** shows the plot that relates the *J* function to Water Saturation. Data are mostly scattered but is possible to notice linear trend of grouped data below 10% water saturation. The colored points indicate 4 main reservoirs used as reference for the models (R2, R3, R4 and R5 in **Fig. 13**). The scattered points shown in the circle indicate top and bottom parts of some reservoirs which log measurements are affected by the shale bed below and upper, the so called shoulder effects (see, for example, resistivity logs for R2, indicated by blue points, **Fig. 13**). Black and rose points with J values greater than 4 indicates reservoirs or parts of the reservoirs affected by shoulder effect whilst those grouped points with more than 85% water saturated indicates thin beds between the colored reservoir points. The water Saturation (SW_JF) was computed based on log-log plot of water Saturation against J function. The plot on the right shows the logarithm correlation of both data. The red line represents the best linear fit of the data trend. The result is verified by using the equation below (see appendix for details), which final coefficients were -0.257494 and -1.02107 for A and B, respectively. The final Saturation height curve is show in the **Fig. 8.**

$$Sw = 10^{(A - B \log_{10} J)} = 10^{A} J^{-B} \tag{17}$$

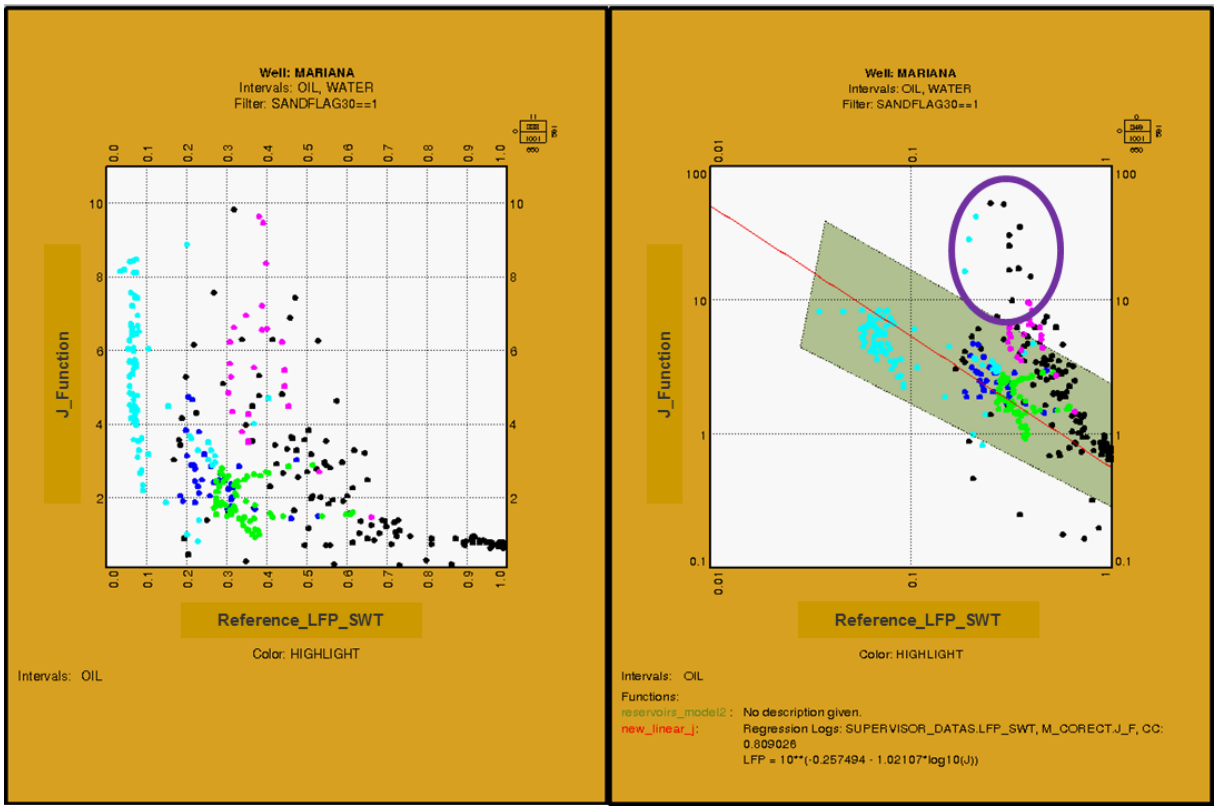

Figure 7 - The Leverett and reference Sw correlation on linear and logarithm scale. The Purple Circle indicates part of the reservoirs that are affected by shoulder effect.

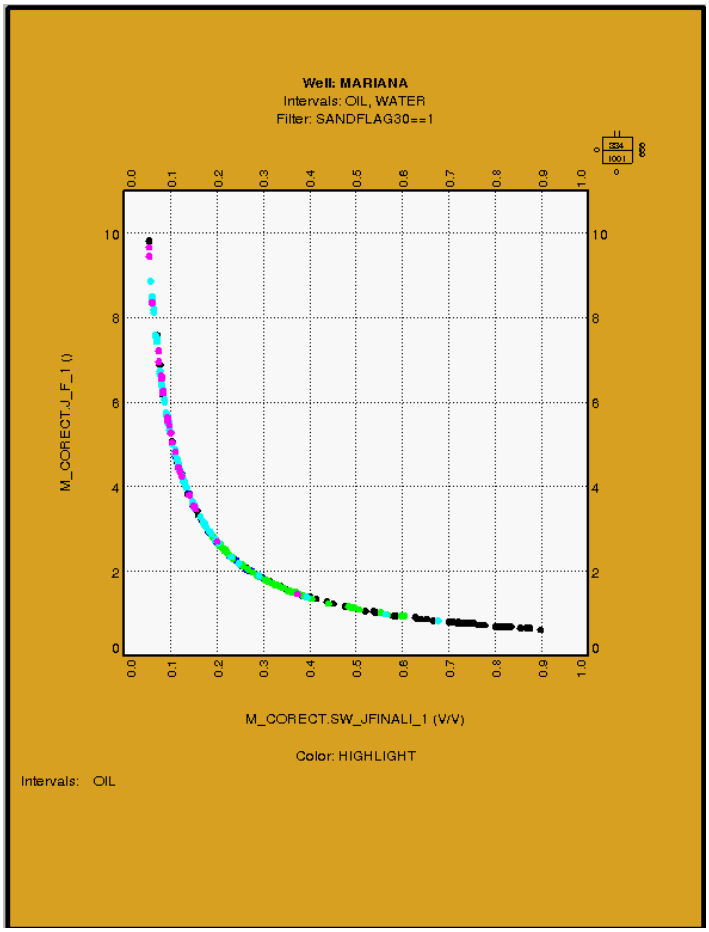

Figure 8 - The final SwH curve computed from Leverett

8.2 Cuddy Function (FOIL)

The bulk volume of water (BVW) was computed using the equation (12). **Fig. 9** shows BVW plotted against HAFWL, which FWL is at 3976 (MD), and the general data trend. Observations of the colored and black data points stated previously in the Leverett Function are valid here, likewise. Similarly, a log-log plot of BVW against HAFWL shows a possible linear data trend. The regression line indicate that the BVW can be related to HAFWL by using equation (14) which coefficients are 1.4425 and -1.70629 for A and B, respectively. The final bulk volume from this correlation (BVW2) and the curve that shows its relation to the HAFWL is shown in **Fig. 10**

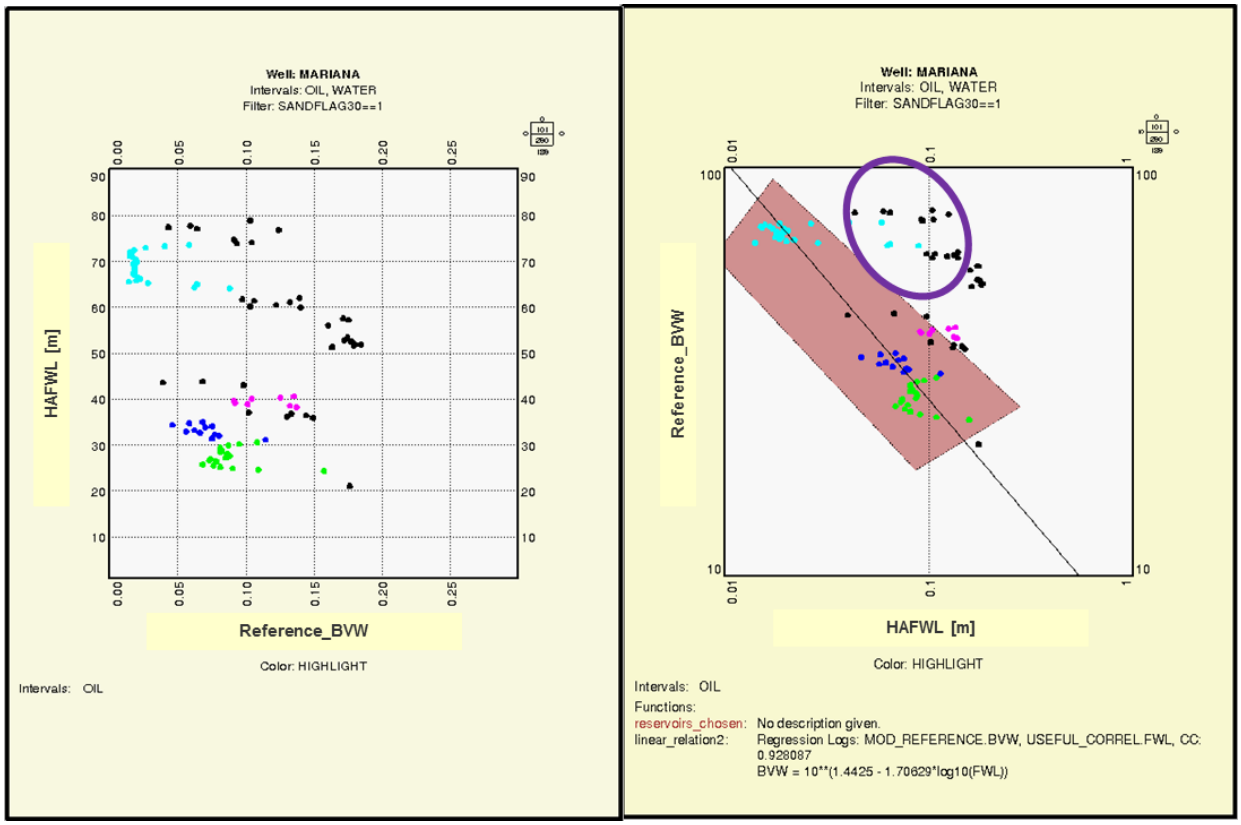

Figure 9 - The reference BVW versus HAFWL on linear scale. The same correlation is made on logarithm scale. The Purple Circle indicates part of the reservoirs that are affected by shoulder effect

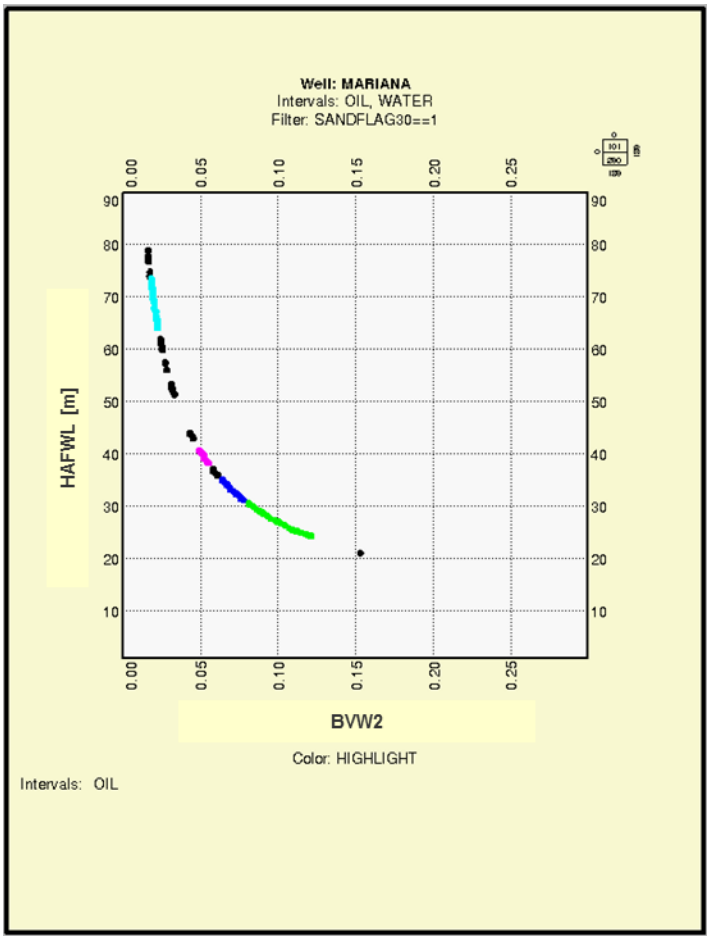

Figure 10 - The final FOIL model.

8.3 Comparison of the Results

For comparison reasons, bulk volume of water (BVW_JF) computed from Sw_J and water saturation curve (SW_Cuddy) computed from BVW1_Cuddy were plotted together with BVW and LFP_SWT, respectively. **Fig. 11** shows that good curves agreement is observed at Capillary Pressure values between 1.0 bar and 1.2 bar (with Sw lower than 10% approximately), corresponding to reservoir 2 (R2) shown in **Fig. 13.** However, at values of capillary pressure below 1bar, the Leverett water saturation tends to underestimate, whilst the one from Cuddy tends to overestimate the water saturation of the reservoir, comparatively to LFP_SWT. Almost the same behavior is noticed when the 3 bulk volume of water are plotted against HAFWL. **Fig.**

12 shows that a reasonably good curve fit can be observed at HAFWL correspondent to Reservoir 2. The same underestimation and overestimation behavior from Leverett and Cuddy curves respectively, is noticed in the bulk volume of water computed at HAFWL below 60m, although below 40m and at BVW greater than 4% BVW_JF seems to be fit better to the reference BVW. A bunch of data from both models agrees that around 5-10% of the fluid volume is retained by small pores and is not displaced under any existing pressure, the so called, irreducible water saturation (EL-Kathib 1995). An entire overview of the 3 curves trend is observed when no filter is applied, as shown in **Fig. 11**.

A primary interpretation of both models applied is that for this particular well, they can be very suitable for calculating the Sw of the well. At parts of the reservoir which capillary pressure values vary between 1.0 and 1.4 with very low water-saturated can be expected reliable results. However, for lower capillary pressure values a correction factor may be needed to achieve better results.

Fig. 13 also shows that regardless the fact that the Cuddy water saturation model virtually does not take into account the properties of the rock for the calculation of the Sw, a conspicuous reasonable curve fit can be noticed. The curve also has less variation and average water saturation variation trend seems to be better assumed by the Cuddy curve than Leverett. However, seems like higher curve mismatch is seen at R4 and R5, comparatively to Sw computed by using Leverett.

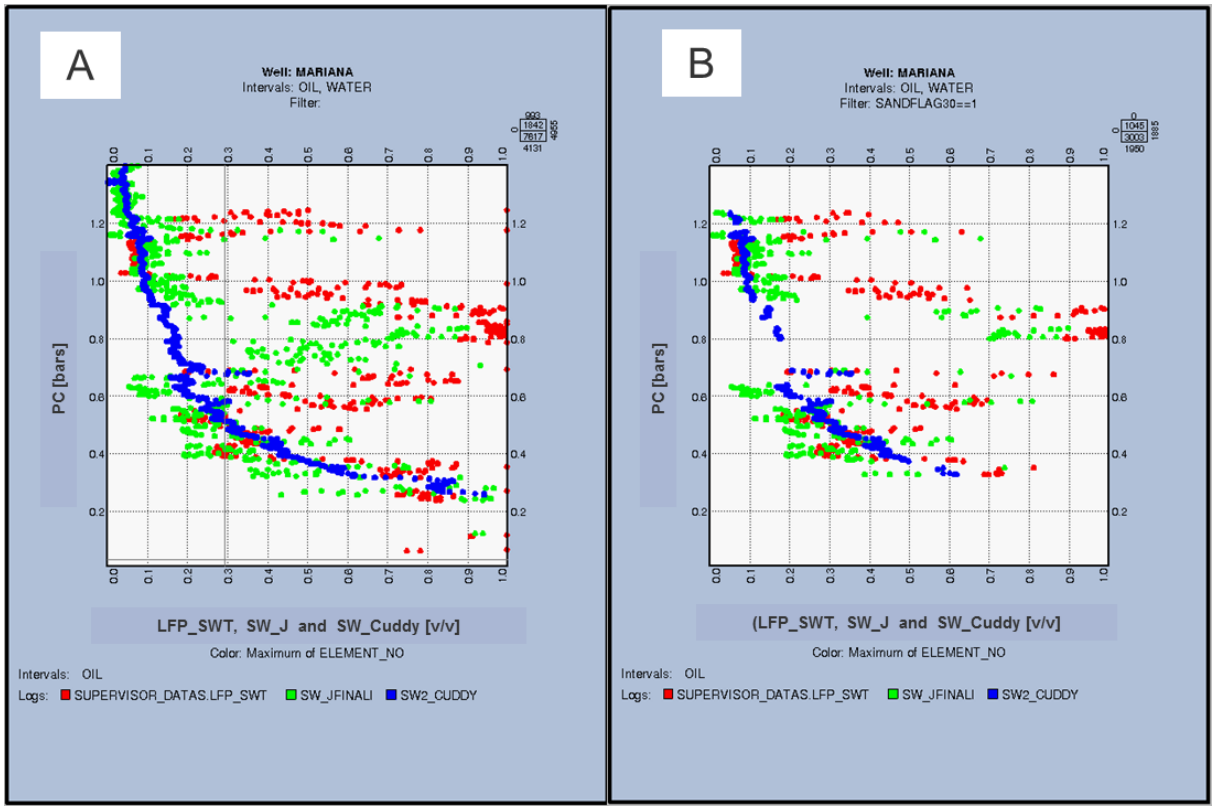

Figure 11 - Crossplots of the 3 Sw models with the capillary pressure. A-without filter; B-with Sandflag filter

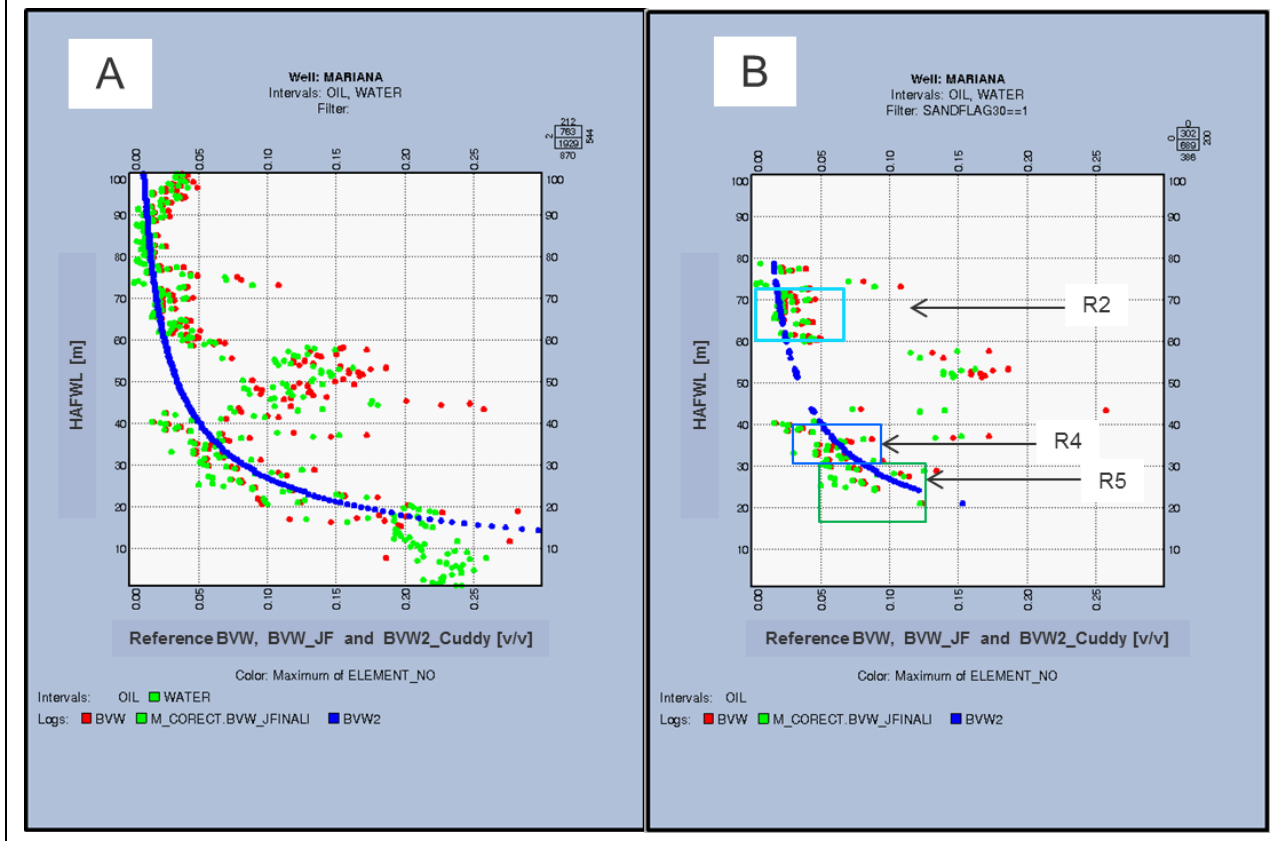

Figure 12 - Comparisons of the Sw plotted against the Height Above Free Water Level. A- Without Filter; B-with Sandflag filter

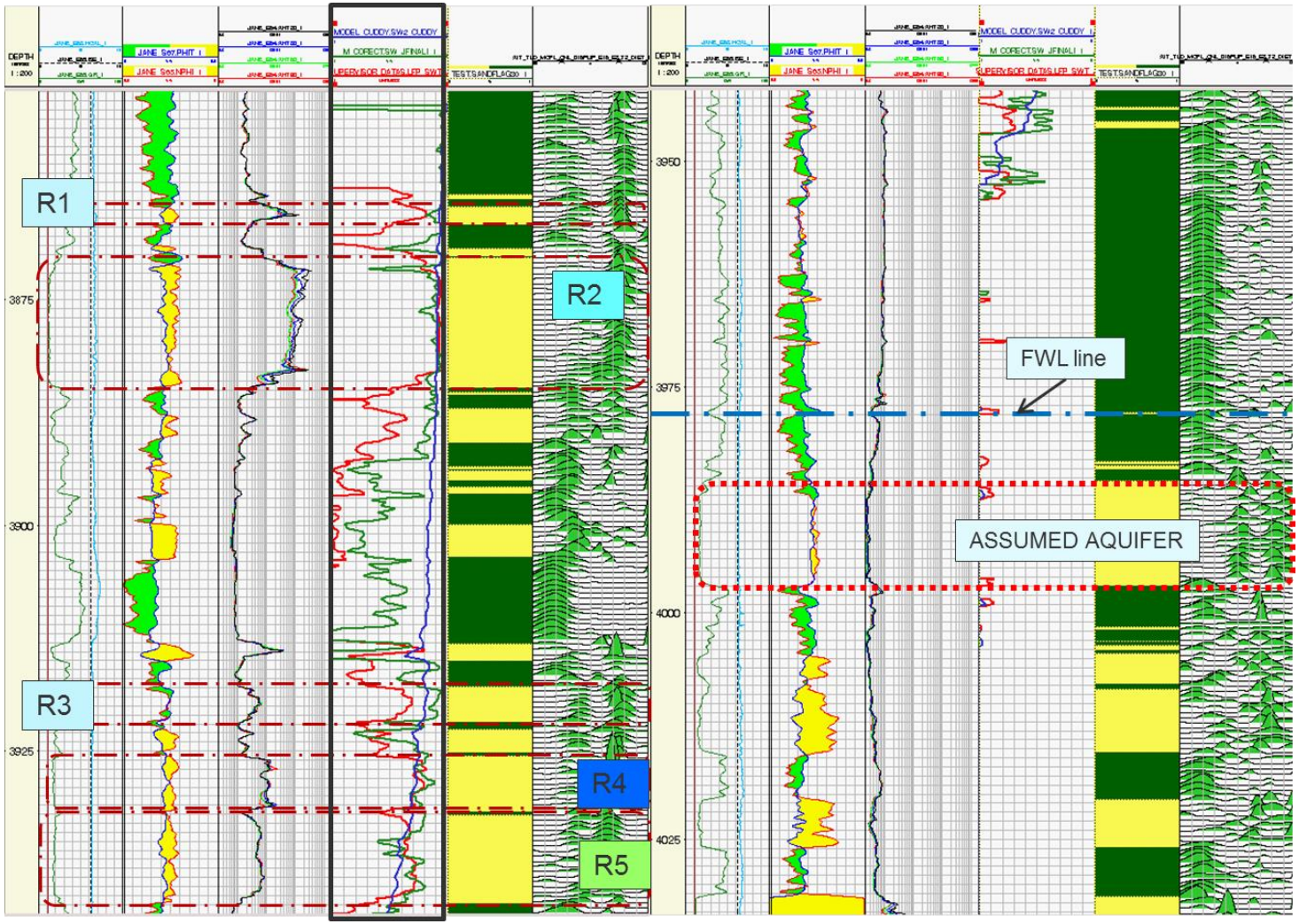

Figure 13 – comparison of the final Saturations models (the highlighted track). The colors represent the reservoirs used as base for models

9 Discussion

An important but critical point of the Leverett approach used here is the fact that it can be highly controlled by the rock quality factor, the square root of permeability-porosity ratio (Humble Oil and Refining Company, 1961). There is no logging tool that measures the rock permeability and the lab method still shows to give more accurate measurement and this fact affect the accuracy of the permeability curve. Although the permeability used here was correlated from core permeability, there were not enough data points for the best curve fit; Different results may be expected if a better permeability log is used. But regarding porosity, the curve should remain unaffected as the log porosity calibrated from core showed to be reliable. This problem is avoided by Cuddy´s model that showed to be virtually porosity independent and could be useful for comparisons purpose, when available permeability is not trustful. In his paper, Cuddy performed his experiment in a brine-gas reservoir with a very clear WGC and stated that results can be affected if it is not clear. However, seems to be that although the analysis made here reflects different reservoir conditions (brine-oil) and the contact is far of being clear, that fact does not affected much the results, as no much difference is seen from the reference Sw curve (at least for lower values of Sw in R2). The overestimation trend from Cuddy method was already addressed by Harrison and Jiang (2001) for Brine-Oil reservoirs. This over estimation reflects better when calculation of volumetric Hydrocarbon in place is performed.

A common inference of J(Sw) is the fact that a better curve fit is expected from less scattered data point and this may imply a good porosity-permeability agreement (Humble Oil and Refining Company, 1961). It seems to be very suitable for this particular well, as the permeability and Porosity shows good agreement and especially in R3, where the data present better grouped. The fact that the models were adjusted to those parts of the well where logs results are less affected by shoulder effect (though R2 is affected) and the R3 is included, could be also taken into consideration but, it does not affect the results, as no much difference is seen from the reference Sw curve.

Furthermore, the models could also be adjusted to, and compared with, some shaly sand water saturation approaches, then the volume of shale calculated could be removed/reduced from the

assumed clean sands (which Vsh<0.3) and best results could be achieved. However, most of the Vshale water saturation models remain considered as empirical or not scientifically reliable, as Schlumberger and Indonesia. Lab data such as BQv (Equivalent conductivity of exchange cations), used for those models based on CEC (such as Waxman-Smits), considered scientifically reliable were not accessible. For this work, the intention was to avoid underpinning scientific question of the models whence first approach and verification of the reference Sw was by using Archie. Furthermore, the Rw calculated (0,029) when placed with water-bearing formation temperature (~70ºC) in a formation water salinity crossplot gives salinity value closely to ranges where Archie´s equation could still be a reliable approach for the water saturation adjustment. Probably, further studies and model improvement could be expected if some Lab data from this particular well were obtainable.

Finally, the SwH models applied could be used for improvement of STOIIP of the reservoir. The great importance of the Saturation-Height modeling functions is that they can be extrapolated to zones away from the well and aid on prediction of the saturation anywhere in the reservoir. This means that if more valuable data from different wells, such as porosity, permeability, Capillary pressure resultant from Lab analysis, the SwH models could become more realistic and the problem of accessibility to formation data away from the well could be minimized by extrapolating the models to these unreachable zones, but of course taking into considerations the natural limitations of the models.

10 Conclusion

Two saturation-height models equation were applied to the well Mariana to compute water saturations which showed to give reliable results.

Both models showed that an improvement of the water saturation results using the models could be made if correction factors be used in zones with water saturation greater than 13% or capillary pressure bellow 1 bar. For the Foil model an overestimated preventing correction factor should be suitable, whilst for the Leverett J(Sw) should be used an underestimate preventing correction factor.

The SwH models applied, if improved, could be used to estimate saturations by extrapolation into unreachable zones of the field.

11 Bibliography

Cuddy, S.; Allinson, G. and Steele, R., 1993, *"A simple convincing model for calculating water saturations in southern North Sea gas fields"*, SPWLA 34th Annual Logging Symposium, June 13-16

Doveton, John H. 2014, "*Principles of Mathematical Petrophysics"*, editor Oxford University Press, 2014, International Association for Mathematical Geosciences studies in Mathematical Geosciences no. 9, Chapter 2, pag 43-51

Ellis, D.V. and Singer, J.M., 2008., "*Well Logging for Earth Scientists"*, 2nd Edition, Chapter 23.2 Published by Springer, 2008, pag 654-671

Hamada, G.M., SPE, AL-Awad, M.N. and Alsughayer, College of Engeneering, King Saud University, Saudi Arabia., "*variable saturation exponent effect on the determination of hydrocarbon saturation*"., SPE 77887, 2001

Ibrahim, A.; Bassiouni, Z. and Desbrandes, R., 1992, "*Determination of Relative Permeability Curves in Tight Gas Sands Using Log Data*". SPWLA 33rd Annual Logging Symposium, June 14-17.

Leverett, M.C., 1941. "*Capillary Behavior in Porous Solid*", Society of Petroleum Engineers, SPE

Leverett, M.C., 1942. "*Dimensional-model Studies of Oil-field Behavior*", Society of Petroleum Engineers, SPE

Osisanya, S.O., Tiab, D. and Elgaghah, S.A., "*A New Approach for Obtaining J-function in Clean and Shaly Reservoirs Using in Situ Measurements*" The Petroleum Society, paper 98-14

Skelt, C., Harrison B., 1995, "*An Integrated Approach to Saturation Height Analysis*" SPWLA 36th Annual Logging Symposium, June 26-29.

Wiltgen, N. A.; Le Calvez, J. and Owen k., 2003*., "Methods of Saturation Modeling Using Capillary Pressure Averaging and Pseudos"* SPWLA 44th Annual Logging Symposium, June 22-25.

Guy Huntley humble Oil, L. and Oklahoma City Oil Company., 1961, "*The correlation of capillary pressure and electric log data to establish the saturation exponent"*, SPWLA, Oklahoma

Pascoal, Dario E. T., 2015 " *Evaluation of Diagenetic Minerals Effects on The Porosity Logging Tools on Well Mariana, Offshore Congo Basin*", NTNU, semester project 2014

Harrison, B. and Jing, X.D., 2001, "*Saturation Height Methods and Their Impact on Volumetric Hydrocarbon in Place Estimates*", Society of Petroleum Engineers, SPE,

Walther, H.C., 1968, "*Saturation from Logs Laboratory Measurements of Logging Parameters*" Society of Petroleum Engineers, SPE

12 Appendix

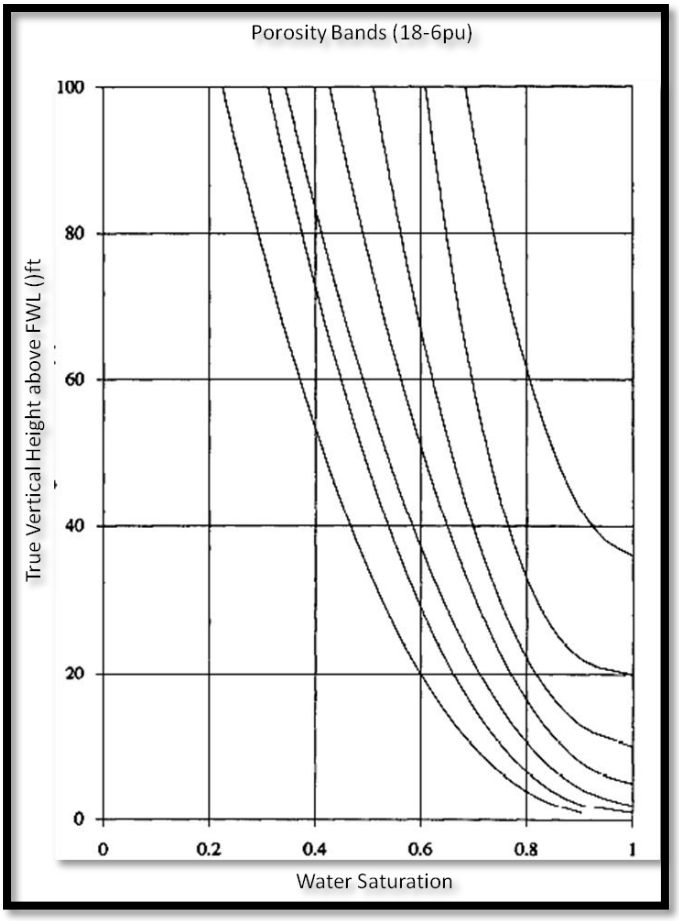

Figure 14 - Examples of Curves from the Classical functions (Cuddy et al., 1993)

Showing the porosity independence of Cuddy model using Archie's formula when m=n=2:

$$BWV = Sw * \emptyset$$

And replacing the Sw by Archie's Sw

$$BVW = \sqrt{\frac{Rw * a}{\emptyset^2 * Rt}} * \emptyset$$

which can be also written as:

$$BVW = \sqrt{\frac{Rw * a}{Rt}} * \frac{\emptyset}{\emptyset}$$

Then, the final result shows the Bulk volume of water calculated independent of the porosity:

$$BVW = \sqrt{\frac{Rw * a}{Rt}}$$

Equation for verification of the Leverett Function

$$J(Sw) = \frac{\alpha}{Sw^{\beta}}$$

$$Sw = \left(\frac{J}{\alpha}\right)^{-1/\beta}$$

$$\log_{10} Sw = \frac{-1}{\beta}\log_{10}\left(\frac{J}{\alpha}\right)$$

$$\log_{10} Sw = \frac{\log_{10}\alpha}{\beta} - \frac{\log_{10} J}{\beta}$$

$$Sw = 10^{\left(\frac{\log_{10}\alpha}{\beta} - \frac{\log_{10} J}{\beta}\right)}$$

$$Sw = 10^{(a - b\log_{10} J)} = 10^{a} J^{-b}$$

Parameters *a* and *b* can be found by regression of *Sw* vs. *J* in the petrophysical software.

Note that $b = 1/\beta$ and $a = \log_{10}(\alpha)/\beta$.

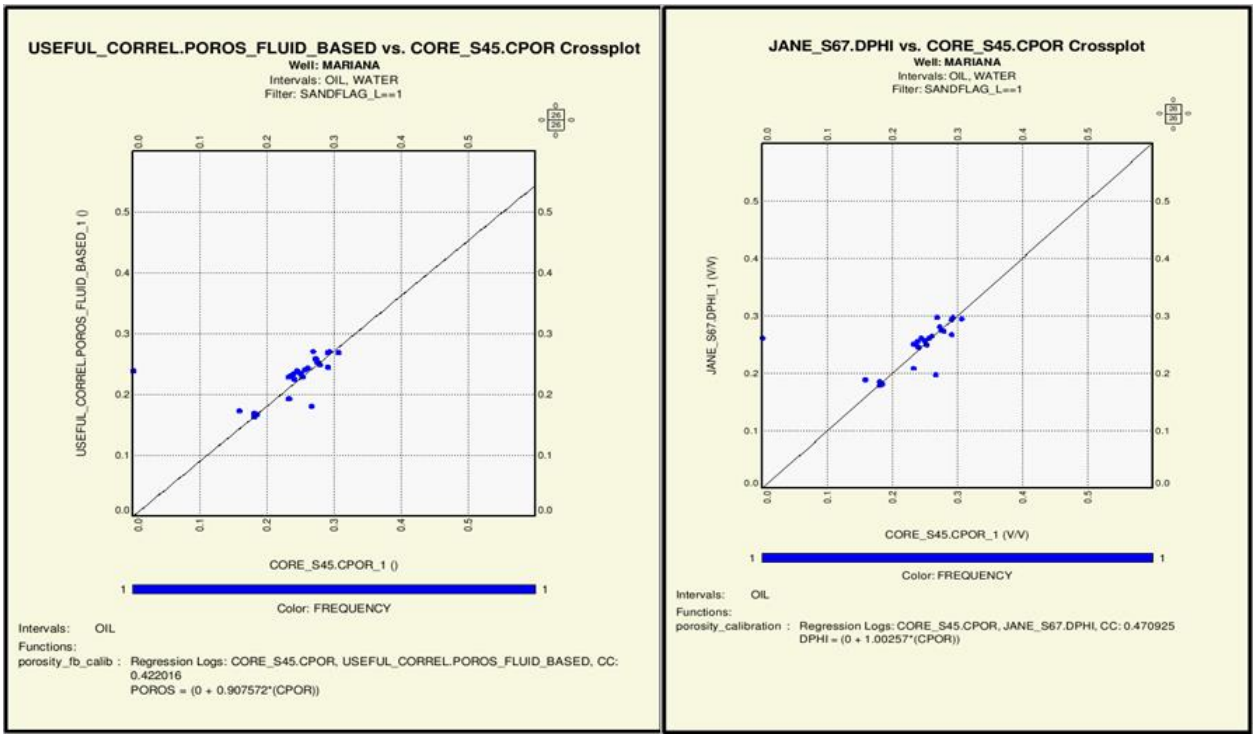

Figure 15 - Plot showing the calibration of two porosity log curves to verify the LFP_PHITT used for computation of SwH models

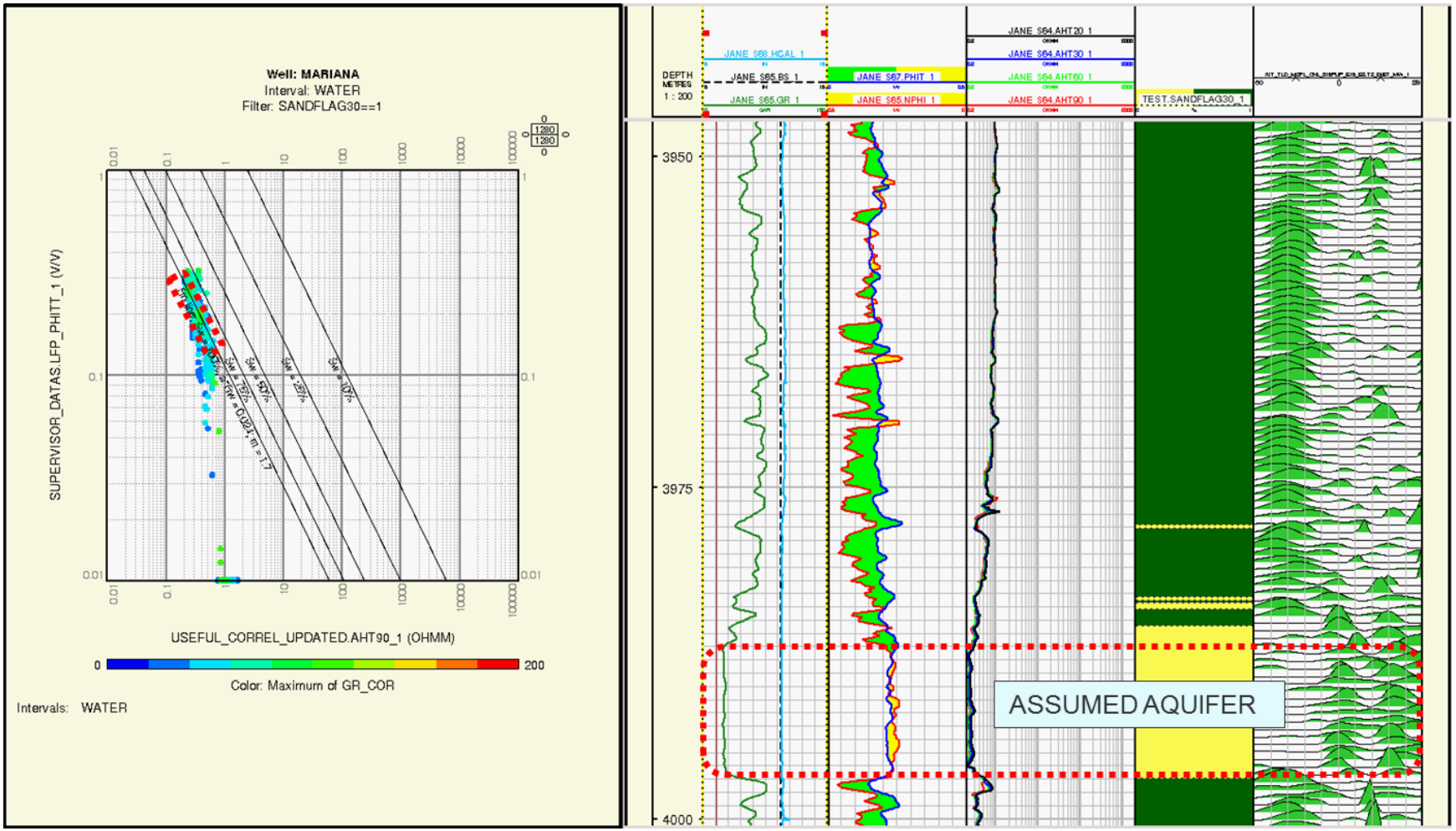

Figure 16 - Picket plot showing the water resistivity in the zone of interest. The red marks in the picket plot represents the zone in the Layout marked likewise.

Mnemonics for fig. 4

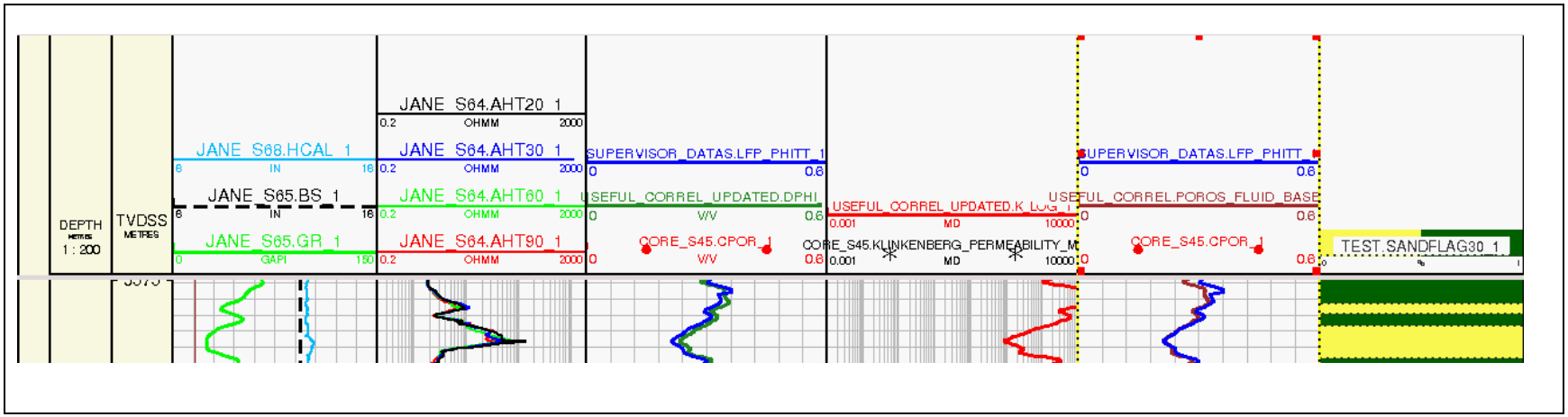

Mnemonics for fig. 6

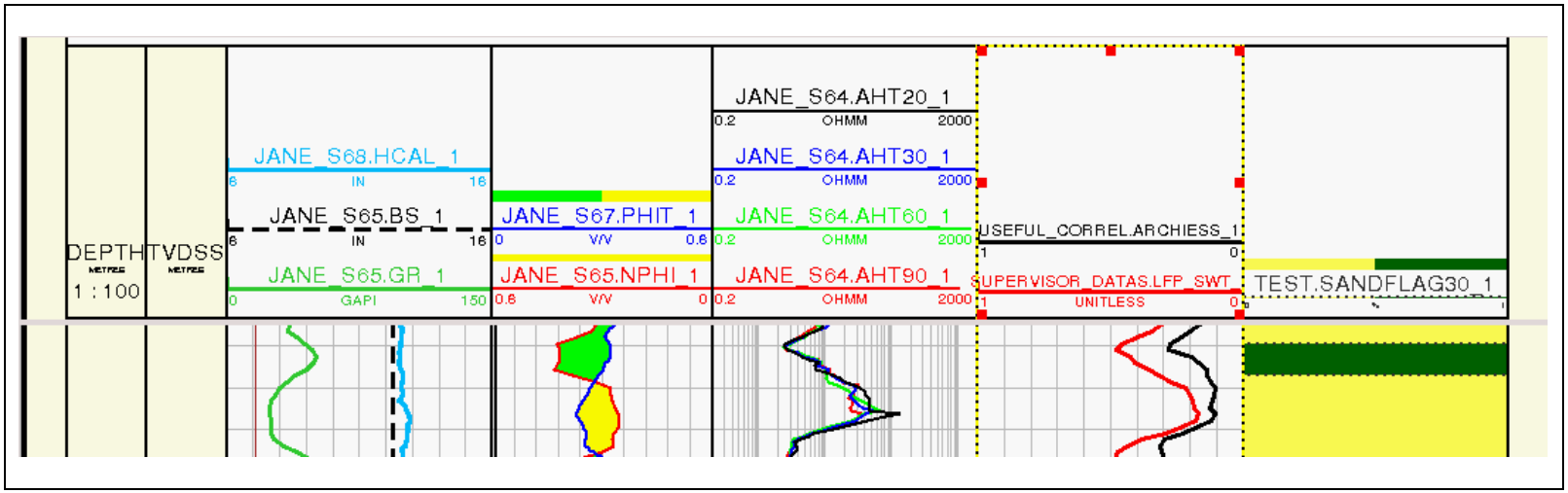

Mnemonics for fig. 13